J Mater Sci: Mater Electron (2009) 20:1255–1259
DOI 10.1007/s10854-009-9861-z

Growth and characterization of ZnO films on (11-20) sapphire substrates by atomic layer deposition using DEZn and N_2O

Kuo-Yi Yen · Kuang-Pi Liu · Jyh-Rong Gong · Kuen-Yau Tsai · Dong-Yuan Lyu · Tai-Yuan Lin · Guo-Yu Ni · Far-Wen Jih

Received: 17 October 2008 / Accepted: 17 February 2009 / Published online: 4 March 2009

Abstract Zinc oxide (ZnO) films were grown on (11-20) sapphire substrates at 600 °C by atomic layer deposition (ALD) using diethylzinc (DEZn) and nitrous oxide (N_2O). A ZnO buffer layer was deposited at low temperature (LT) prior to the growth of a bulk ZnO film for a typical growth run. In some cases, buffer-layer annealing or post-annealing treatments were employed to optimize ZnO growth. Based on the experimental results of X-ray diffractometry (XRD) and transmission electron microscopy (TEM), all the as-grown ZnO films were found to show *c*-axis preferred orientation with co-existence of $<1\text{-}100>_{ZnO}\|<1\text{-}100>_{sapphire}$ and $<11\text{-}20>_{ZnO}\|<1\text{-}100>_{sapphire}$ relationships in the (0001)ZnO/(11-20)sapphire hetero-interface. Typical room temperature (RT) photoluminescence (PL) spectrum of the as-grown ZnO film shows only near band edge (NBE) emissions without defect luminescence. ZnO films with improved quality were achieved by post-annealing or buffer-layer annealing treatments. In particular, buffer-layer annealing was found to improve the crystalline and optical properties of a ZnO film substantially.

K.-Y. Yen · K.-P. Liu · J.-R. Gong · K.-Y. Tsai
Department of Physics, National Chung Hsing University, Taichung 402, Taiwan, ROC

J.-R. Gong (✉)
Institute of Nanoscience, National Chung Hsing University, Taichung 402, Taiwan, ROC
e-mail: jrgong@phys.nchu.edu.tw

D.-Y. Lyu · T.-Y. Lin
Institute of Optoelectronic Sciences, National Taiwan Ocean University, Keelung 202, Taiwan, ROC

G.-Y. Ni · F.-W. Jih
Materials and Electro-Optics Research Division, Chung Shan Institute of Science and Technology, Taoyuan 325, Taiwan, ROC

1 Introduction

ZnO is a direct wide band gap semiconductor material having wurtzite structure with an energy gap of 3.3 eV at RT. Due to its exciton binding energy being larger than that of GaN [1, 2], the wide band-gap oxide has recently been considered as a potential substitute of GaN for opto-electronic applications. Several techniques were currently employed for ZnO growth including metal-organic chemical vapor deposition (MOCVD) [3], pulsed-laser deposition (PLD) [4], molecular-beam epitaxy (MBE) [5], vapor–liquid–solid epitaxy (VLSE) [6, 7], and atomic layer deposition (ALD) [8]. Recently, ALD has manifested itself as an important technique for the growth of nano-scale gate dielectrics in the metal-oxide-semiconductor field-effect transistors (MOSFETs) and conformal side-wall deposition of dielectrics inside high aspect ratio trenches in nano-electronics fabrication [9]. We have also reported ALD growth of high optical quality ZnO films on (0001) plane sapphire substrates by buffer-layer annealing (or post-annealing treatment) lately [10]. Annealing treatments under certain conditions were found to enable formation of ZnO nanowires. Previous evaluation also showed that, for a (0001) plane-oriented ZnO film grown on the (11-20) sapphire substrate, the mismatches along the $<11\text{-}20>_{ZnO}$ and $<1\text{-}100>_{ZnO}$ directions were far less than the mismatch of 19% for a (0001) plane-oriented ZnO film deposited on the (0001) sapphire substrate [11]. Whether or not the reduced lattice-mismatch between (0001) ZnO film and (11-20)

sapphire substrate affects the properties of the ZnO film remains as an interesting issue to be explored.

In this paper, we present the characteristics of ALD-grown ZnO films on (11-20) sapphire substrates using DEZn and N_2O. It was found that the crystalline and optical properties of the ZnO film could be improved by certain annealing treatments.

2 Experimental

ZnO films, about 0.3 μm in thickness, were prepared on (11-20) Al_2O_3 substrates at 600 °C in an inductively heated quartz reactor operated at atmospheric pressure. ALD growth of ZnO proceeded by exposing the substrate alternatively to DEZn and N_2O fluxes. The (11-20) sapphire substrate was solvent-cleaned first, followed by hot-etched in an HCl/H_3PO_4 (3:1) solution for 5 min, rinsed with de-ionized water, and blow-dried with N_2 gas before loading. For a typical growth run of the ZnO film deposited on (11-20) sapphire substrate under certain buffer-layer deposition temperature, a 40 nm-thick LT-ZnO buffer layer was first deposited at 100, 200, 300, 400, or 500 °C, followed by the growth of a 0.3 μm-thick ZnO film at 600 °C. For a buffer-layer annealed ZnO film, prior to the deposition of a 0.3 μm-thick ZnO film at 600 °C, the LT-ZnO buffer layer was annealed at 800 °C for 2 min under N_2O exposure. In the case of a post-annealed ZnO film, after the deposition of a 0.3 μm-thick ZnO film, the film was post-annealed at 1000 °C for 1 h under N_2O overpressure. In both post-annealed and buffer-layer annealed ZnO samples, LT-ZnO buffer layers were prepared at 300 °C (or 400 °C) with the subsequent deposition of 0.3 μm-thick ZnO films being conducted at 600 °C.

A four-point probe equipment and a MAC-MXP^3 X-ray diffractometer were employed for revealing conductive and structural characteristics of the ZnO films. Photoluminescence (PL) measurements of ZnO films were conducted by using the 325 nm excitation of a He–Cd laser as the light source. A JEOL 1200 EX II transmission electron microscope (TEM) was employed to identify the nano-structures of the ZnO films. TEM samples were prepared by using a Gatan 600-DIF Ar ion milling equipment.

3 Results and discussion

Based on the results of four-point probe measurements, the resistivity of a typical as-grown ZnO film was found in the range of low 10^{-2} Ω-cm. Figure 1 exhibits typical θ-to-2θ X-ray diffraction plots of ZnO films grown on the (11-20) sapphire substrates with LT-ZnO buffer layers being prepared at 100, 200, 300, 400, and 500 °C, respectively. In this case, the thicknesses of ZnO films remain at 0.3 μm. It appears that only the $(0002)_{ZnO}$ and $(0004)_{ZnO}$ diffracted peaks of the ZnO film were observed although the (11-20) peak of the sapphire substrate was also identified in all the X-ray plots. According to the θ-to-2θ X-ray diffraction data, it is clear that the (0001) plane of a ZnO film is oriented in parallel to the (11-20) plane of the sapphire substrate.

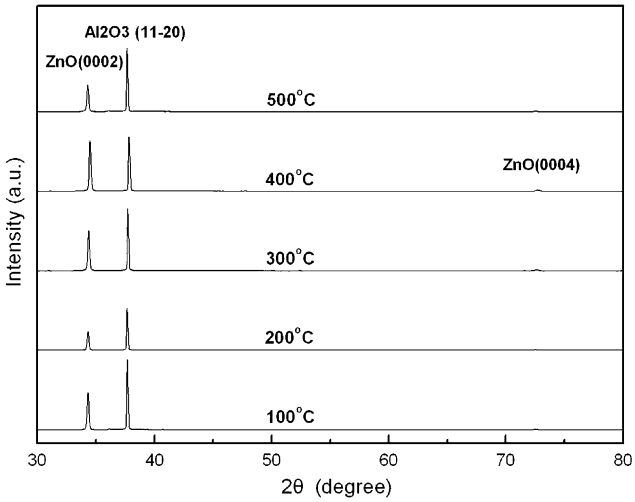

Fig. 1 Typical θ-to-2θ X-ray diffraction spectra of the as-grown ZnO films on (11-20) sapphire substrates by ALD having LT-ZnO buffer layers being deposited at various temperatures

Unlike the XRD results, the cross-sectional TEM (XTEM) observations, however, indicate that all the as-grown ZnO films are not monocrystalline in nature. Instead, there are two types of orientation relationships between ZnO and sapphire in the (0001)ZnO/(11-20) sapphire hetero-interface. Figure 2a–c reveal a typical XTEM image, the corresponding diffraction pattern and an indexed schematic of the diffracted spots, respectively, of a typical as-grown ZnO film. In this case, the electron beam is parallel to the $[1\text{-}100]_{sapphire}$ zone axis of the sapphire substrate, and the indexed schematic highlights both the cross marks (x) and dot signs (·) representing the diffracted spots observed along $[1\text{-}100]_{ZnO}$ and $[11\text{-}20]_{ZnO}$ zone axes of ZnO, respectively. It appears that the c-axis prefer-oriented ZnO domains exhibit either $<1\text{-}100>_{ZnO}\|<1\text{-}100>_{sapphire}$ or $<11\text{-}20>_{ZnO}\|<1\text{-}100>_{sapphire}$ orientation relationship in the (0001)ZnO/(11-20)sapphire hetero-interface. The $<1\text{-}100>_{ZnO}\|<1\text{-}100>_{sapphire}$ and $<11\text{-}20>_{ZnO}\|<1\text{-}100>_{sapphire}$ relationships were previously reported in the literatures [11, 12]. Figure 3a and b show schematics of the atomic arrangements of (0001) ZnO on (11-20) sapphire with $[1\text{-}100]_{ZnO}\ \|[1\text{-}100]_{sapphire}$ and $[11\text{-}20]_{ZnO}\|[1\text{-}100]_{sapphire}$ orientation dependence, respectively. A rough estimation shows that the lattice mismatches of the atomic arrangement, as depicted in Fig. 3b, along $<1\text{-}100>_{ZnO}$ and $<11\text{-}20>_{ZnO}$ directions are

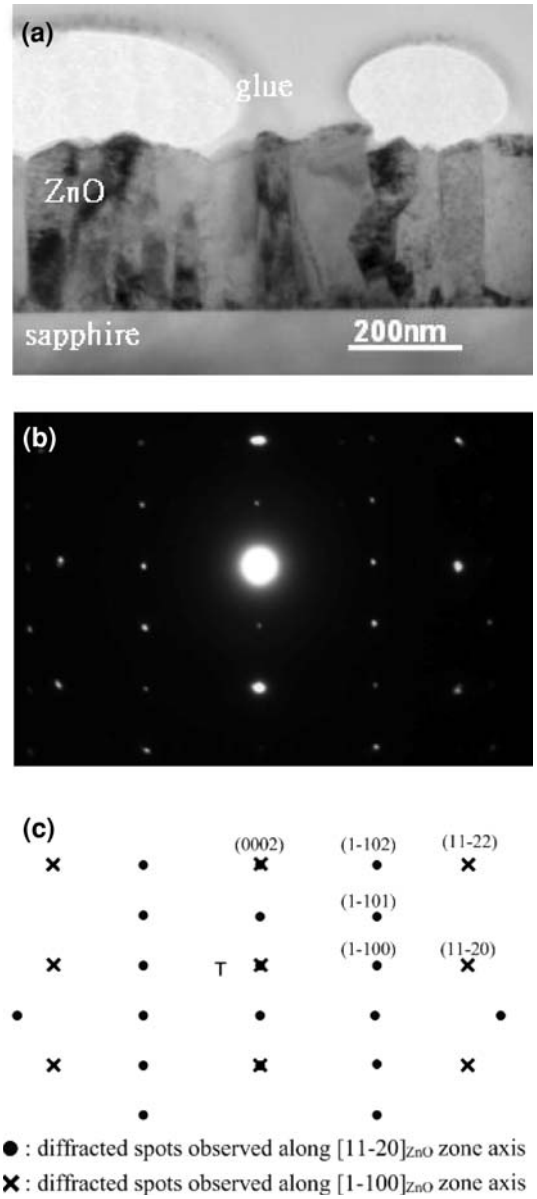

Fig. 2 A typical **a** XTEM image along with **b** its diffraction pattern and **c** an indexed schematic of the diffraction spots of a ZnO film grown at 600 °C having a 300 °C-deposited ZnO buffer layer without annealing treatment. Both *cross marks* (x) and *dot signs* (·) represent the diffracted spots observed along $[1\text{-}100]_{ZnO}$ and $[11\text{-}20]_{ZnO}$ zone axes of ZnO, respectively.(Note that the e-beam is parallel to the $[1\text{-}100]_{sapphire}$ zone axis of sapphire.)

1.5 and 18.3 %, respectively, which, on the average, are larger than the lattice mismatches of 0.5 and 2.4 % along $<11\text{-}20>_{ZnO}$ and $<1\text{-}100>_{ZnO}$ directions of the atomic configuration as shown in Fig. 3a. It is believed that low buffer layer deposition temperature enables accommodation of large lattice mismatch so that the as-grown ZnO film tends to form the above-mentioned two types of orientation relationships simultaneously in the (0001)ZnO/(11-20)sapphire heterostructure.

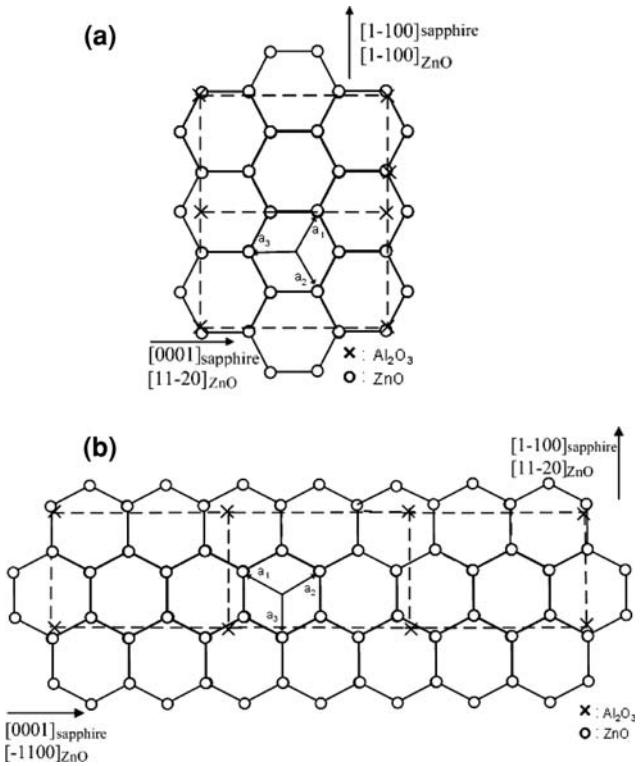

Fig. 3 Schematics of the atomic arrangements in ZnO and sapphire of the $(0001)_{ZnO}/(11\text{-}20)_{sapphire}$ heterostructure with **a** $<1\text{-}100>_{ZnO}\|<1\text{-}100>_{sapphire}$ and **b** $<11\text{-}20>_{ZnO}\|<1\text{-}100>_{sapphire}$ orientation relationships, respectively

The results of PL measurements showed that there was almost no green luminescence except the NBE emissions for all the as-grown ZnO films without annealing treatment. The green luminescence was previously reported to be originated from oxygen vacancies, and was frequently observed in ZnO [13]. Thus, we tentatively consider that sufficient N_2O overpressure, in this study, is helpful to reduce the density of oxygen vacancies in the ZnO films so that only the NBE PL emissions were observed for all the ZnO films. Despite the XRD results are quite similar among the as-grown ZnO samples, the optical properties of ZnO films were found being sensitive to buffer-layer deposition temperature. Figure 4 depicts plots of FWHM and peak intensity of the RT NBE PL emissions of the as-grown ZnO film versus buffer layer deposition temperature. It is apparent that the narrowest FWHM and the strongest peak intensity of the RT NBE PL emissions occur at the ZnO sample having a buffer layer deposition temperature of 300 °C. This result again confirms that a reduced buffer layer deposition temperature is helpful to accommodate the lattice mismatches between (0001) ZnO film and (11-20) sapphire substrate, but further decrement in buffer layer process temperature may also sacrifice the structural and optical quality of the ZnO film deposited subsequently. On the other hand, an elevated buffer layer

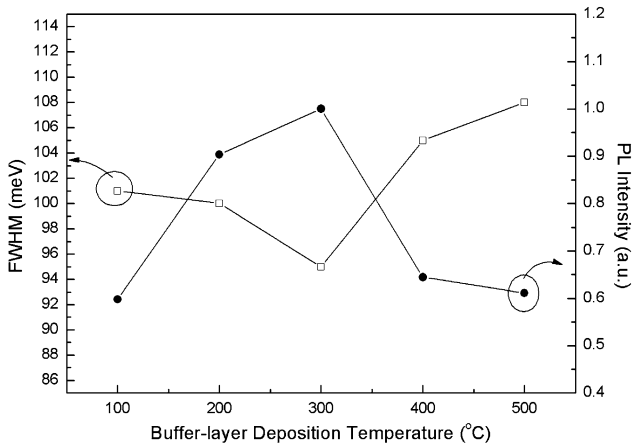

Fig. 4 Plots of RT NBE PL peak intensity and linewidth versus buffer layer deposition temperature of the ALD-grown ZnO films on (11-20) sapphire substrates without buffer-layer annealing treatment

deposition temperature tends to cause uneven ZnO buffer layer which results in the deterioration of surface morphology of the ZnO film grown at the later stage. Thus, an optimized buffer-layer deposition temperature at 300 °C is realized.

In order to improve the crystalline and optical properties of a ZnO film, we conducted additional thermal processes including post-annealing and buffer-layer annealing treatments. Figure 5 shows plots of RT PL spectra of the ZnO films grown at 600 °C with LT-ZnO buffer layers being deposited at 300 and 400 °C, respectively, followed by annealing at 800 °C for 2 min under N_2O overpressure. It was found that a reduction of LT-ZnO buffer layer deposition temperature from 400 to 300 °C tended to result in considerable intensity increment and FWHM decrement

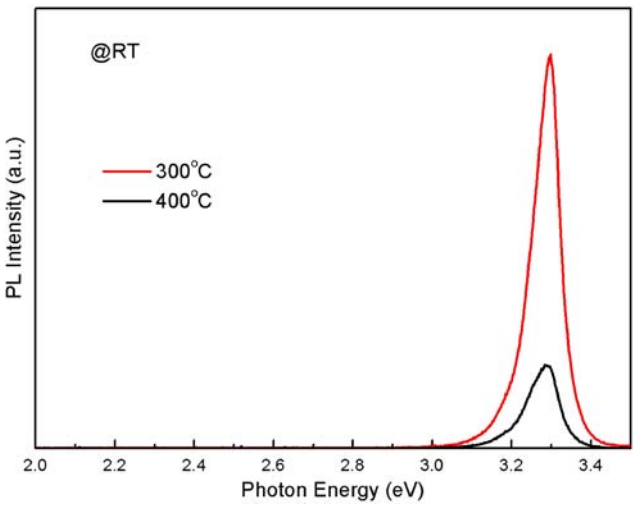

Fig. 5 RT PL spectra of the ZnO films grown at 600 °C having LT-ZnO buffer layers being deposited at 300 and 400 °C, respectively, with buffer-layers being annealed at 800 °C for 2 min under N_2O overpressure

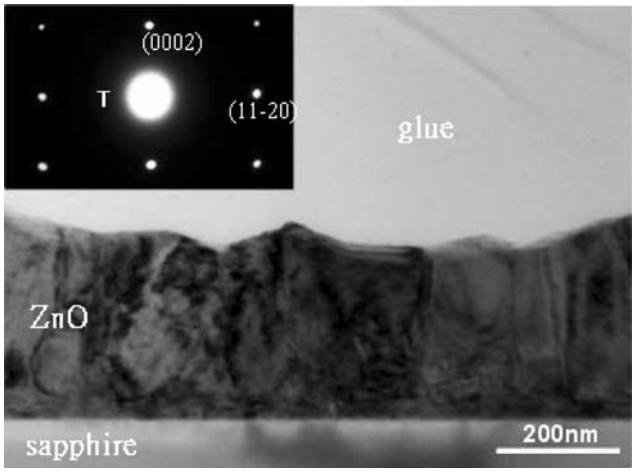

Fig. 6 A typical XTEM image with an inset of diffraction pattern of a ZnO film with buffer-layer being annealed at 800 °C for 2 min under N_2O overpressure

(from 94 to 78 meV) of the RT NBE PL emissions of a buffer-layer annealed ZnO film. Such a result agrees quite well with the results given in Fig. 4. It is considered that the thickness of a LT-ZnO buffer layer is more uniform for a 300 °C-deposited LT-ZnO buffer layer than that of a 400 °C-deposited LT-ZnO buffer layer. Thus, re-crystallization of the 300 °C-deposited LT-ZnO buffer layer is more efficient than that of the 400 °C-deposited LT-ZnO buffer layer under the same buffer-layer annealing condition. Accordingly, the structural and optical characteristics of the buffer-layer annealed ZnO film having a 300 °C-deposited LT-ZnO buffer layer are expected to be better than those of the buffer-layer annealed ZnO film having a 400 °C-deposited LT-ZnO buffer layer.

Figure 6 exhibits a XTEM image along with an inset showing the corresponding electron diffraction pattern of the buffer-layer annealed ZnO film with LT-ZnO buffer layer being deposited at 300 °C. It is evident that large ZnO grains can be achieved by conducting buffer-layer annealing treatment. In this case, (0001) plane ZnO was found to deposit on the (11-20) plane sapphire substrate only with its $[1\text{-}100]_{ZnO}$ being parallel to $[1\text{-}100]_{sapphire}$. No other orientation relationship was observed between ZnO and sapphire. Comparing with the XTEM results of the ZnO films without annealing treatment (Fig. 2a–c), it is clear that buffer-layer annealing treatment enables coalescence among ZnO nano-crystals and results in the unique $[1\text{-}100]_{ZnO} \parallel [1\text{-}100]_{sapphire}$ orientation correspondence between ZnO and sapphire in the (0001)ZnO/(11-20)sapphire heterointerface. Note that the presence of $[1\text{-}100]_{ZnO} \parallel [1\text{-}100]_{sapphire}$ orientation relationship between ZnO and sapphire allows to minimize the strain energy of the (0001)ZnO/(11-20)sapphire heterostructure because it is the most energetically favorable orientation

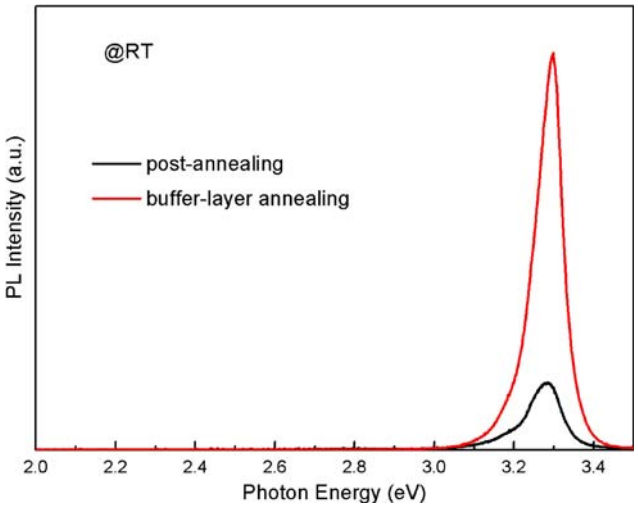

Fig. 7 Plots of the RT NBE PL spectra of the 1,000 °C post-annealed and 800 °C buffer-layer annealed ZnO films with LT-buffer layers being prepared at 300 °C

correspondence between (0001) ZnO and (11-20) sapphire due to its small lattice mismatches.

Figure 7 shows plots of the RT PL spectra of buffer-layer annealed and post-annealed ZnO films. In this case, both 40 nm-thick LT-ZnO buffer layer and 0.3 μm-thick ZnO films were deposited at 300 and 600 °C, respectively, with the buffer-layer annealed ZnO sample being buffer-layer annealed at 800 °C for 2 min and the post-annealed sample being post-annealed at 1000 °C for 1 h. Apparently, the peak intensity of the RT NBE PL emissions of the buffer-layer annealed ZnO film is much stronger than that of the post-annealed ZnO film. It is considered that annealing treatment at an elevated temperature provides much more efficient re-crystallization for the 40 nm-thick LT-ZnO buffer layer than the 0.3 μm-thick ZnO film so that the RT NBE PL intensity is strongly enhanced in the buffer-layer annealed ZnO film. This explains the fact that buffer-layer annealing treatment is much more efficient than post-annealing treatment in improving the optical quality of the ALD-grown ZnO films on (11-20) sapphire substrates in this study.

4 Conclusions

We conducted investigations to explore the properties of ZnO films grown on (11-20) sapphire substrates by ALD using LT-ZnO buffer layers. Both XRD and XTEM studies revealed that the as-grown ZnO films showed two kinds of orientation relationships in the (0001)ZnO/(11-20)sapphire hetero-interface. Post-annealing and buffer-layer annealing treatments were found to enhance the optical properties of the ZnO films. In particular, remarkable improvement in crystallinity and enhancement in NBE PL intensity were observed in the buffer-layer annealed ZnO films.

Acknowledgments This work was supported in part by the National Science Council of Taiwan, Republic of China with contract numbers NSC94-2112-M-005-014 and NSC97-2112-M-005-004-MY3.

References

1. K. Tamura, A. Ohtomo, Y. Osaka, T. Makino, Y. Segawa, M. Sumiya, S. Fuke, H. Koinuma, M. Kawasaki, J. Cryst. Growth **214/215**, 59 (2000). doi:10.1016/S0022-0248(00)00059-2
2. Y. Chen, H. Ko, S. Hong, T. Yao, Y. Segawa, J. Cryst. Growth **214/215**, 87 (2000). doi:10.1016/S0022-0248(00)00072-5
3. S. Liu, J.J. Wu, Mater. Res. Soc. Symp. Proc. **703**, 241 (2002)
4. A. Sasaki, W. Hara, A. Matsuda, N. Tateda, S. Otaka, S. Akiba, Appl. Phys. Lett. **86**, 231911 (2005). doi:10.1063/1.1947378
5. H. Tampo, A. Yamada, P. Fons, H. Shibata, K. Matsubara, K. Iwat, S. Niki, Appl. Phys. Lett. **84**, 4412 (2004). doi:10.1063/1.1758295
6. M.H. Huang, Y. Wu, H. Feick, N. Tran, E. Weber, P. Yang, Adv. Mater. **13**, 113 (2001). doi:10.1002/1521-4095(200101)13:2<113::AID-ADMA113>3.0.CO;2-H
7. Y.C. Kong, D.P. Yu, B. Zhang, W. Fang, S.Q. Feng, Appl. Phys. Lett. **78**, 407 (2001). doi:10.1063/1.1342050
8. K. Saito, Y. Yamamoto, A. Matsuda, S. Izumi, T. Uchino, K. Ishida, K. Takahashi, Phys. Stat. Sol. (b). **229**, 925 (2002). doi:10.1002/1521-3951(200201)229:2<925::AID-PSSB925>3.0.CO;2-7
9. C.Y. Chang, S.M. Sze, *ULSI devices* (Wiley, New York, 2000)
10. P.Y. Lin, J.R. Gong, P.C. Li, T.Y. Lin, D.Y. Lyu, D.Y. Lin, H.J. Lin, T.C. Li, K.J. Chang, W.J. Lin, J. Cryst. Growth **310**, 3024 (2008). doi:10.1016/j.jcrysgro.2008.03.016
11. T. Koyama, S.F. Chichibu, J. Appl. Phys. **95**, 7856 (2000). doi:10.1063/1.1739294
12. P. Fons, K. Iwata, A. Yamada, K. Matsubara, S. Niki, K. Nakahara, T. Tanabe, H. Takasu, Appl. Phys. Lett. **77**, 1801 (2000). doi:10.1063/1.1311603
13. K. Vanheusden, C.H. Seager, W.L. Warren, D.R. Tallant, J.A. Voigt, Appl. Phys. Lett. **68**, 403 (1995). doi:10.1063/1.116699